International Journal of Engineering & Technology, 7 (4.22) (2018) 111-119

International Journal of Engineering & Technology

Website: www.sciencepubco.com/index.php/IJET

Research paper

Comparative Analysis of Model Reference Adaptive Controller in Steam Distillation Process for Essential Oil Extraction System

Nurhani Kasuan[1]*, Mohd Hezri Fazalul Rahiman[2], Mohd Nasir Taib[2], Mohd Hafiz A. Jalil[3], Masmaria Abd Majid[1], Farah Yasmin Abd Rahman[2]

[1]Faculty of Electrical Engineering, Universiti Teknologi MARA, Pasir Gudang, Johor, MALAYSIA
[2] Faculty of Electrical Engineering, Universiti Teknologi MARA, Shah Alam, Selangor MALAYSIA
[3] Faculty of Electrical & Electronic Engineering, Universiti Tun Hussein Onn, Johor MALAYSIA
**Corresponding author E-mail: nurhani924@johor.uitm.edu.my*

Abstract

This paper aims to study the Model Reference Adaptive Controller using MIT-Rule and Lyapunov applied in a pilot-scale steam distillation process. The control objective of MRAC is to regulate steam temperature in the distillation column for essential oil extraction system. A first-order auto-regressive exogenous (ARX) function is derived to represent steam temperature model for numerical experimentation and extended to real-time implementation. During the experiments, the MRAC MIT-Rule and Lyapunov's are tested with and without integral component in the controller structure. It shows that eliminating the integral give stable response and low steady-state error compared to MRAC with the integral. The MRAC–MIT controller has fast response and low SSE and RMSE compared to the MRAC–Lyapunov in both simulation and real-time experimentation.

Keywords: *Model reference adaptive controller, Essential oil extraction, Real-time, Steam distillation.*

1. Introduction

The essential oil from plant materials contains fragile aromatic molecules that can easily be destroyed or modified by changes caused during the extraction process. Even a subtle difference in extraction process conditions can have a significant effect on oil quality. In conventional steam distillation method, high temperatures or extended heat were exposed to botanical plants that can cause thermal degradation in the extracted oil [1, 4-7]. Consequently, the quality of the chemical composition properties of the oil decreases, affecting the aromatic profiles and color of the oil. Numerous researchers made continuous efforts to improve the existing extraction methods and to overcome any shortcomings of the present techniques. Similarly, the drawbacks of conventional extraction techniques motivated the author to embed technological advancements in the respective processes to solve the identifiable problems. Some other drawbacks that have been highlighted in the steam distillation process include the system operating in saturated temperatures [2], and long extraction periods [15, 16], with the common steam distillation process taking from 3 to 8 hours [10-12] depending on the quantity and particle size of the raw materials. In addition, there is no selectivity [4] in steam distillation.

Nevertheless, steam distillation holds several advantages, such as having lower development and operational costs compared to other extraction methods [13], being appropriate for most essential oil extraction [14], and having potential for commercialization [15] due to its reliability in mass oil production. Furthermore, the advantages of steam distillation compared to other distillation methods were mentioned in several previous studies. According to Ozel et al. [16], the relative chemical composition of volatile compounds obtained by steam distillation and superheated water extraction (SWE) were proven to be similar. In fact, steam distillation itself can produce more oil compared to superheated water extraction. Additionally, Scalia et al. [1] revealed that the qualitative profile of essential oils obtained by supercritical fluid extraction (SFE) was comparable with those produced by steam distillation. Indeed, Ammann et al. [15] concluded that, for the chosen study, steam distillation was the most effective technique compared to SFE and SWE. In comparison to supercritical carbon dioxide extraction methods, steam distillation produced a greater yield, and the quality of oil extracted by both methods was similar [3]. The advantages and disadvantages of the steam distillation process highlighted above notwithstanding, in practice, whether in industrial or agricultural activities, the steam distillation method is still preferred. Therefore, the trade-offs regarding the drawbacks of the system remain worthwhile. In this study, the shortcomings identified in the steam distillation system provide areas for improvement. By focusing on research opportunities, these shortcomings can be resolved hypothetically by proposing an advanced temperature controller integrated in steam distillation systems. This also provides a user-defined function that enhances selectivity or options for the system operator. Further, the implementation of an advanced controller is expected to improve system efficiency, which implies shortening the duration of extraction and consequently lowering energy consumption.

The paper is organised as follows. Section 2 briefly describes prototype plant hardware set up and modelling technique of empirical model that applied ARX model structure to represent temperature dynamics. Then, control architecture of MRAC and tuning strategy is explained thoroughly in this Section 3. Results of simulation and real-time of MRAC are shown in Section 4. Section 5 concludes this research finding and highlight some task for future consideration.

2. Plant Proto-type and Modelling

2.1. System Description

A general illustration on temperature controller module of the system is shown in Figure 1. The system consists of a three phase 240-Vac immersion type heater with a power rating of 3kW, microprocessor based 25A ac power controller to drive the heater and temperature sensing modules.

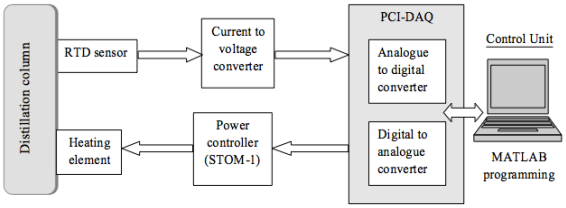

Fig. 1: Block diagram of steam distillation plant, computer and interface.

The sensor is a platinum sensing element i.e. PT100 3-wires type and connected with signal processing circuit with output ranging from 0 to 5V that corresponds to temperatures from 0ºC to 110ºC. The system is using PC-based as control unit. The data acquired using PCI-1711 Advantech data acquisition card to interface between hardware and the computer. MATLAB is used as programming tool for control platform and monitoring of signal responses in to or out from the system. The temperature of the plant is regulated using power controller that generates control signals from 0 to 5Vdc via digital-to-analog converter (DAC) then fed to the heater as an actuator to the plant. The sampling period for the system is 10 seconds. For the software part, MATLAB Real Time Workshop (RTW) is employed.

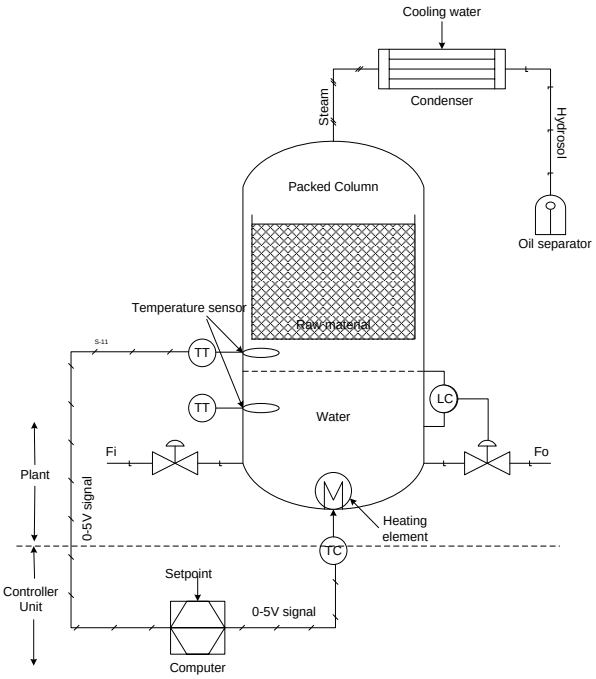

Fig. 2: Steam Distillation Process for Essential OilExtraction

Figure 2 shows a schematic diagram of steam distillation plant that consist of distillation column, packed bed, condenser and heater module. In distillation process prototype, botanical material to be extracted is located at the upper side of the column and 10 litre of water is filled in the column. A heating system with immersion type heater is used to boil the water. As water boiled, steam is produced and passed through the botanical material and escaped with tiny oil molecules to condenser. The condenser will trap the steam and convert it into hydrosol. Hydrosol is the liquid mixture of extracted essential oil and water. The yield or hydrosol, from steam distillation process is deposited in oil separator and the oil will be filtered out.

2.2. System Modelling

Due to lacking of information on mass transfer, equilibrium relationship together with nonlinear interaction and uncertain conditions in the system, the empirical model is sufficient to represent the system via proper experimentation of steam distillation process. The system model expression was derived based on real operation of steam distillation processing plant. For modeling, the output temperature was obtained based on Pseudo Random Binary Sequence (PRBS) signal perturbed into system input. The purpose of PRBS is to trigger or excite the system response at various frequencies. In the study, the PRBS signal is generated by 9-bit shift register with an Exclusive OR gate as shown in Figure 3. The signal is devised as a perturbation signal *u(k)* for the system. The PRBS amplitude is selected to adhere at maximum of 80% from the full scale (4V) when the PRBS signal is 1 and 20% of full scale (1V) when the PRBS signal is at 0.

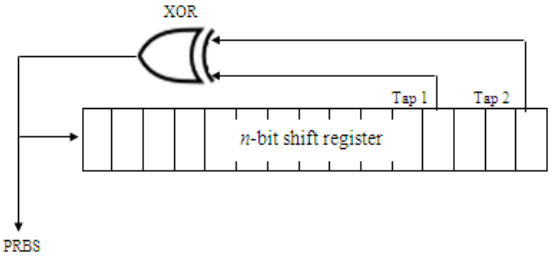

Fig. 3: Realization of PRBS tapping at LFSR with XOR gate at the feedback.

The steam temperature response is represented as *y(t)*. While, *u(t)* is referred to PRBS input signal. The steam temperature for steam distillation process can be well approximated by autoregressive with exogenous (ARX) model structure. The expression for ARX model is written in discrete function as follows;

$$y(t) + a_1 y(t-1) + \cdots + a_{n_a} y(t-n_a) = b_1 u(t-1) + \cdots + b_{n_b} u(t-n_b) + e(t) \quad (1)$$

where the adjustable parameters are stated as:

$$\theta = \left[a_1 \;\; a_2 \ldots \;\; a_{n_a} \;\; b_1 \;\; b_2 \ldots \; b_{n_b}\right]^T \quad (2)$$

The expression of auto regressive part, *A(q) y(t)* is;

$$A(q) = 1 + a_1 q^{-1} + \cdots + a_{n_a} q^{-n_a} \quad (3)$$

Then, expression for exogenous part, *B(q) u(t)* is;

$$B(q) = b_1 q^{-1} + \cdots + b_{n_b} q^{-n_b} \quad (4)$$

where A(q) and B(q) are polynomials for output, *y(t)* and input, *u(t)* terms respectively. While, *e(t)* represents white noise entering the system. *n* is the time delay in the number of sampling time. The chosen sampling time is 10s. The modeling data is divided into two parts and subjected for training and validating the model. The division of input-output data is carried out by using interlacing technique; where odd sequence data meant for training while even sequence data is meant for testing or validating purposes. The approximate ARX mode structure for steam temperature response is a first order function.

In order to identify the unknown parameters of the approximate model structure, the recursive least squares estimation method was been adopted. .

$$\hat{\theta}(t) = \hat{\theta}(t-1) + K(t)[y(t) - \hat{y}(t)] \quad (5)$$

$$K(t) = \frac{P(t-1)\psi(t-1)}{\lambda + \psi^T(t-1)P(t-1)\psi(t-1)} \quad (6)$$

$$P(t) = \frac{1}{\lambda}[I - K(t)\psi^T(t-1)]P(t-1) \quad (7)$$

where ψ and $\hat{\theta}$ are regression matrix and estimated parameters respectively.

$$\psi^T = [y(t-1), u(t-1)] \quad (8)$$

$$\hat{\theta} = [a_1 \;\; b_1 \;]^T \quad (9)$$

P(t) is a 3x3 symmetric matrix where $P(0) = \alpha I_3, \alpha$ is a real large number and λ is a forgetting factor. Therefore the derived estimated model as follows;

$$Y(q) = \frac{0.08088(q^{-1})}{1 - 0.9981(q^{-1})} \quad (10)$$

2.3 Reference Model

A reference model in MRAC is corresponds to desired process performance. The controller is designed to force actual output response to follow model reference. The derivation of model reference signal is by characterizing appropriate process characteristic parameter such as time constant, rise time and final value. In actual practice, suitable temperature profile is determined by user which solely depend on the type of plant material to be extracted. However, for study purposes, the response of model reference is chosen to be;

$$Y_m(q) = \frac{0.02(q^{-1})}{1 - 0.98(q^{-1})} \quad (11)$$

The function is based on typical knowledge of common temperature response. The reference model created to make the response faster with different final value.

Several factors were considered when formulating the reference model, specifically the actuation boundaries that determine the upper and lower limits of process response, and the suitability of the temperature profile for the particular material to be extracted. A dedicated model reference is a first-order function, as stated by Equation by (12). The time constant was set to 220 s with no overshoot. The range of temperature regulation started from began at 70 °C (where steam generation begins) and moved up to

90°C.

$$Y_m = \frac{0.02}{z-0.98} \quad (12)$$

Three curves of model reference were generated using the above model. The maximum temperatures of each response were 80°C, 85°C and 90°C respectively. The models were assumed as the predetermined heating profile for the specific botanical plant to be distillated, as this could prevent temperature saturation during the heating process.
Figure 4 shows three curves of reference models at 80 °C, 85 °C, and 90 °C respectively. These reference models were used in further simulation and the real-time implementation of model-based controllers, MRAC.

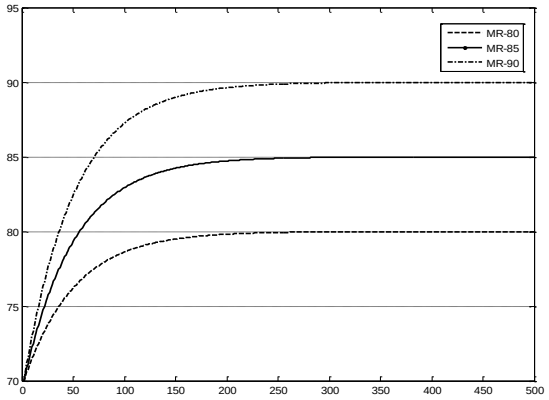

Fig. 4: Model Reference Curves for 80°C, 85 °C, and 90 °C Temperature Regulation

3. Controller Algorithm

3.1 Model Reference Adaptive Control (MRAC)

A general model reference adaptive controller (MRAC) is shown in Figure 5. It consists of three main components, namely controller, reference model, and adjustment mechanism. Two established MRAC structures were used to design the adjustment mechanism: Lyapunov's theorem and the MIT rule. The MIT rule was the first MRAC method, whereas Lyapunov's theorem was used to improve the MRAC–MIT rule structure in terms of stability.

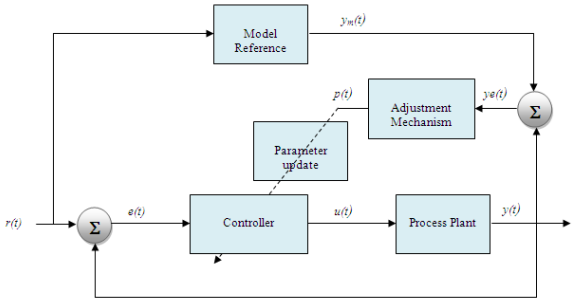

Fig. 5: General Structure of MRAC

In MRAC, the process response y(t), is designed to follow the desired response represented by a model Gm(s). The error signal ye(t) is the difference between model output ym(t) and process response y(t). There is one adjustable parameter θ to be tuned in such a way that the loss function J(θ) is minimized. The loss function is given as

$$J(\theta) = \frac{1}{2}e^2$$

3.2 MRAC using Lyapunov's theorem

The first-order MRAC is based on Lyapunov's stability theorem (MRAC–Lyapunov); the desired response and process are given by (13) and (14) respectively [17]:

$$\frac{dy_m}{dt} = -a_m y_m + b_m u_c \quad (13)$$

$$\frac{dy}{dt} = -ay + bu \quad (14)$$

The controller response, u, and error signal, e, are described by the following equations:

$$u = \theta_1 u_c - \theta_2 y \quad (15)$$

$$e = y - y_m \quad (16)$$

where θ_1 and θ_2 are chosen to be

$$\theta_1 = \theta_1^0 = \frac{b_m}{b} \quad (17)$$

$$\theta_2 = \theta_2^0 = \frac{a_m - a}{b} \quad (18)$$

The differential equation for t he error is given by

$$\frac{de}{dt} = -a_m e - (b\theta_2 + a - a_m)y + (b\theta_1 - b_m)u_c \quad (19)$$

By considering the loss function, the parameter adjustment mechanism is constructed such that the parameters of θ1 and θ2 will converge to their desired values. Thus, the adaptation rules is given as [17]

$$\frac{d\theta_1}{dt} = -\gamma u_c e \quad (20)$$

$$\frac{d\theta_2}{dt} = \gamma y e \quad (21)$$

where γ is a positive constant. Figure 3.10 illustrates the block diagram of MRAC that is based on LyapunovLyapunov's theory for a first-order system.

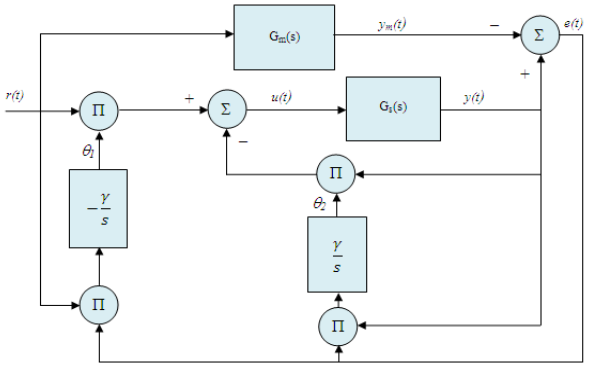

Fig. 6: Model Reference Adaptive Controller using Lyapunov's Rule [17]

3.3 MRAC using MIT-Rule

The desired response and process response in Equation (13) and (14) are the derivation of the first-order MRAC based on the MIT rule (MRAC–MIT). The controller response, error signal, and parameter functions are similar to (15) to (18). The output of the closed-loop system, y, is derived as

$$y = \frac{b\theta_1}{p + a + b\theta_2} u_c \tag{22}$$

The adjustment mechanism for the MIT rule finally is formulated as

$$\frac{d\theta_1}{dt} = -\gamma \left(\frac{a_m}{p + a_m} u_c \right) e \tag{23}$$

$$\frac{d\theta_2}{dt} = \gamma \left(\frac{a_m}{p + a_m} y \right) e \tag{24}$$

where p is the differential operator. Figure 7 illustrates the block diagram of MRAC based on the MIT rule for a first-order system.

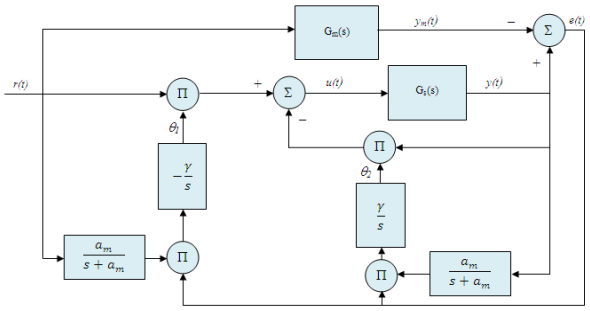

Fig. 7: Model Reference Adaptive Controller using the MIT Rule [17]

3.4 Implementation of MRAC

The initial step in designing MRAC was to derive MRAC functions based on the order of the system. In this research, the steam temperature involved was a first-order system, and the MRAC–MIT and MRAC–Lyapunov were generated based on the first-order model.

Figure 8 illustrates the Simulink block of the MRAC controller structure. The difference between the MIT-rule and Lyapunov's theorem can be seen in the adaptation law where control output u and plant output yp from the MIT rule are connected to the model reference (MR) function in the block, as shown in Figure 9.

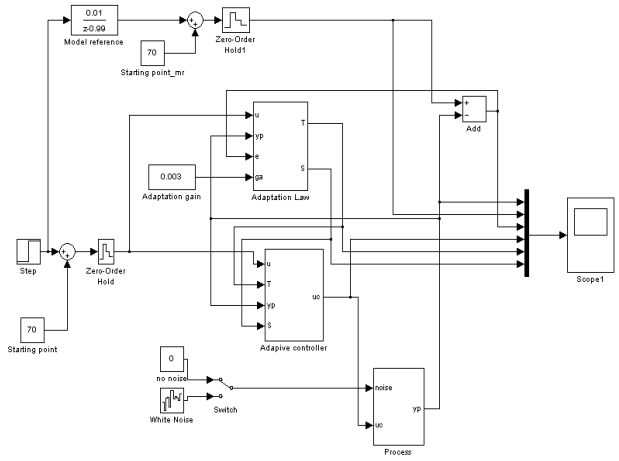

Fig. 8: MRAC Structure in Simulink Block

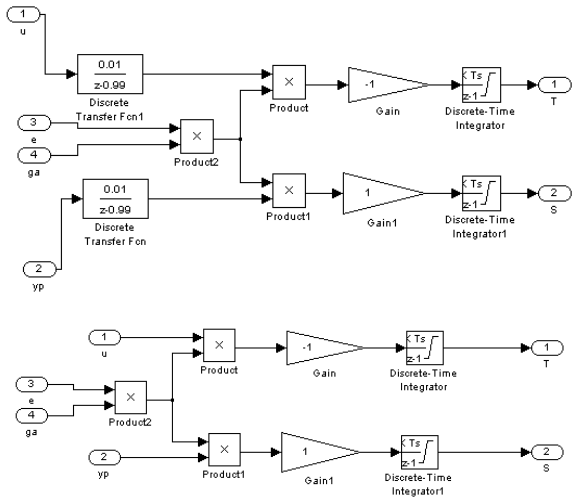

Fig. 9: Simulink Model of Adaptation Law MRAC Structure: (a) MIT Rule, (b) Lyapunov's Theorem

The value of adaptation gain γ was initialized (*refer to Section 4.1- Parameter Tuning*). Convergence of the process response to model output is influenced greatly by adaptation gain. Therefore, it is important to select an appropriate adaptation gain value. Intuitively, small gain value is expected to execute slow convergence, while large gain is expected to cause a faster convergence rate. The experiment was conducted by means of numerical experimentation to obtain the optimum value of adaptation gain. As the experiment established, the process was run in a real-time environment. The adaptation gain might vary from the simulation, but it can be adjusted accordingly to obtain the true value.

4. Results & Discussion

4.1 Parameter Tuning

Initially, the adaptation gain (AG) and integral gain (IG) were tuned to get minimum value SSE and RMSE. There are 2 conditions of MRAC structure were tested i.e. with integral and without integral.

Table 1: The Effects of Integral Limits on the Performance of MRAC (Lyapunov's Theorem and MIT Rule) Controlled Scheme during Simulation

Experiment	Adaptation gain (AG)	Integral gain (IG)	Integral	Error			Stability	Figure
				SSE	RMSE	SSC		
A	100	1	with	3760.76	1.94	400.00	Unstable	y
B	10	1		3760.76	1.94	400.00		
C	1	1		3760.76	1.94	400.00		
D	0.1	1		3760.76	1.94	400.00		
E	0.01	1		3760.76	1.94	400.00		
F	0.001	1		3760.76	1.94	400.00		
G	0.001	10		3760.76	1.94	400.00		y
H	0.001	0.1		3788.92	1.95	210.72		
I	0.001	0.01		3547.29	1.88	24.79		y
J	0.001	0.001		7849.99	2.80	1.15		
K	100	1	without	63.30	0.25	5500.00	Stable	y
L	10	1		63.30	0.25	5500.00		
M	1	1		63.30	0.25	5500.00		
N	0.1	1		63.11	0.25	5463.76		
O	0.01	1		47.97	0.22	4281.26		
P	0.001	1		34.33	0.19	1034.98		
Q	0.003	1		32.79	0.18	2202.71		y
R	0.0001	1		279.57	0.53	38.15		y
S	0.003	10		57.75	0.24	4898.59		y
T	0.003	0.1		52.68	0.23	308.02		
U	0.003	0.01		33.83	0.18	1151.59		
V	0.003	0.001		2502.46	1.58	3.13		y

From Table 1, the experiments without integral conditions achieved stable response and minimum error (SSE & RMSE). The tuned value of AG and IG were 0.003 and 1.0 respectively. Figure 10 shows temperature response in tracking MR function. Error SSE and RMSE obtained were smallest at 32.79 and 0.18 respectively (*refer Table 1 in Experiment Q*).

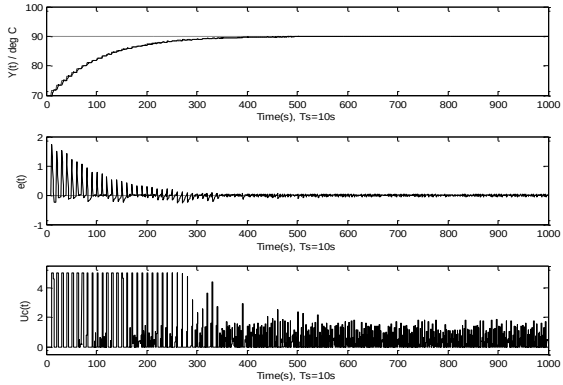

Fig. 10: Temperature response, Error and Controller Output when value of AG= 0.003 and IG=1.0.

4.2 Simulation Results of MRAC–Lyapunov and MRAC–MIT

The simulation of MRAC–Lyapunov and MRAC–MIT was conducted where the MRAC–Lyapunov Experiment were labelled as A1 - A6 and MRAC–MIT labelled as B1 – B6 .

Table 2: The Effects of Integral Limits on the Performance of MRAC (Lyapunov's Theorem and MIT Rule) Controlled Scheme during Simulation

Exp.	Integrator Limit		Performance		
	P_{lower}	P_{upper}	SSE	RMSE	SSC
A1	-inf	Inf	4966.164	2.228	1651.785
A2	-1	1	1103.294	1.050	1770.659
A3	-0.1	0.1	498.799	0.706	1638.480
A4	-0.01	0.01	37.358	0.193	508.162
A5	-0.001	0.001	25527.036	5.052	23.245
A6	Directly eliminated		43.929	0.210	1534.679
B1	-inf	Inf	5181.453	2.276	1607.947
B2	-1	1	991.598	0.996	1707.780
B3	-0.1	0.1	538.210	0.734	1652.731
B4	-0.01	0.01	36.940	0.192	508.841
B5	-0.001	0.001	25527.036	5.052	23.245
B6	Directly eliminated		39.604	0.199	1470.350

Table 2 shows that the absence of integral gives lowest RMSE values (43.929 and 39.604) and SSE values (0.210 and 0.199) for Experiments A6 and B6 respectively. Although the integral was removed from the MRAC structure, the control system was able to execute good output performance and stable response.
Figure 11 shows the simulated process response for Experiments A1, A4, and A6 in tracking steam temperature at 80 °C. Setting the boundaries for the integral limits yielded significant improvement to the process response. However, eliminating the integral showed even better steady-state error compared to MRAC with the integral.

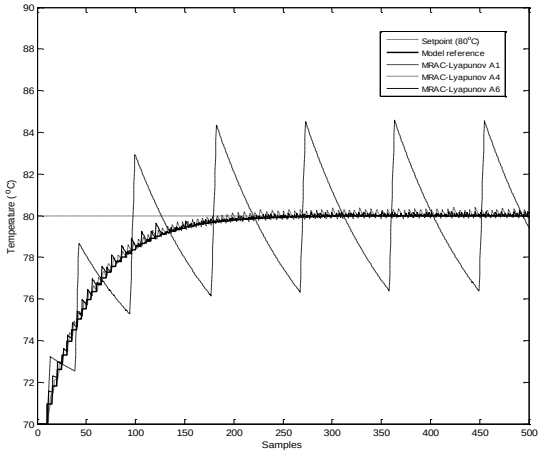

Fig. 11: Simulation of MRAC–Lyapunov Scheme

Figure 12 shows the simulated process responses for Experiments B1, B4, and B6 for MRAC–MIT in the tracking reference model of steam temperature at the 80 °C set point. The results are comparable to MRAC–Lyapunov. The response apparently improves as the boundaries for the integrals are set lower, while eliminating the integral showed improved steady-state error compared to MRAC with integrals.

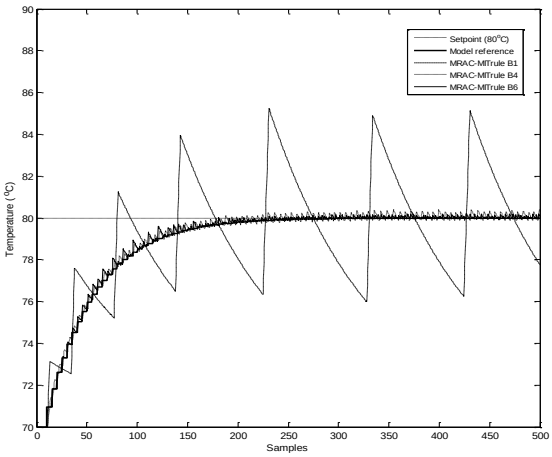

Fig. 12: Simulation of MRAC based on MIT-rule Scheme

4.3 Real-time Performance of MRAC–Lyapunov and MRAC–MIT

The simulated performance of MRAC (Lyapunov and MIT) was validated using the real-time experiment of the steam distillation process. Table 3 shows controller performance of response accuracy and control effort as integral limits change. Experiments A1_RT to A6_RT correspond to real-time MRAC–Lyapunov, while Experiments B1_RT to B6_RT correspond to real-time MRAC–MIT.

Table 3: The Effects of Integral Limits on the Performance of MRAC (Lyapunov and MIT): Controlled Scheme in Real-time Implementation

Exp.	Integrator Limit		Performance		
	P_{lower}	P_{upper}	SSE	RMSE	SSC
A1_RT	-inf	Inf	7284.498	2.766	22150.000
A2_RT	-1	1	3731.219	1.932	17549.310
A3_RT	-0.1	0.1	7256.990	2.693	16691.810
A4_RT	-0.01	0.01	Damping—too slow		
A5_RT	-0.001	0.001	Damping—too slow		
A6_RT	Directly eliminated		1918.776	1.385	15696.570
B1_RT	-inf	Inf	4604.362	2.146	15300.000
B2_RT	-1	1	5985.314	2.446	18006.212
B3_RT	-0.1	0.1	3389.948	1.841	16530.279
B4_RT	-0.01	0.01	Damping—too slow		
B5_RT	-0.001	0.001	Damping—too slow		
B6_RT	Directly eliminated		2453.159	1.566	14899.990

From the result above, the lowest RMSE and SSE were obtained when the integral was directly eliminated (Experiments A6_RT and B6_RT). However, when integral limits were present and set to smaller values, it damped down the process response. Figure 13 and 14 illustrate the real-time process response based on MRAC–Lyapunov and MRAC–MIT respectively.

In Figure 13, the limit of the integral is set to infinity (Experiment A1_RT), and the response indicates a large oscillation with an interval of ± 4 °C with respect to the set point. As the integral limit was adjusted to a smaller boundary, ± 0.1 (Experiment A3_RT), the output yielded a slow tracking response, and it oscillated within ± 1 °C about the set point. It can be seen that the process output is improved when the integral is removed (Experiment A6_RT). The tracking capability of the response is quite fast, and a lower oscillation amplitude occurs in Experiments A1_RT and A3_RT.

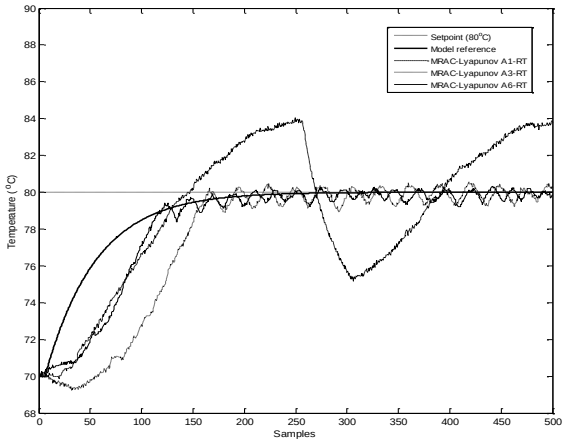

Fig. 13: Process Output using Real-time MRAC–Lyapunov Control Scheme

In experiment B1_RT where the integral was set to infinity, large oscillations occurred, as can be seen in Figure 14. The MIT-rule led to faster oscillations compared to the previous experiment, A1_RT (using Lyapunov's structure), with the amplitude of oscillation for both responses about the same, that is, ± 4 °C with respect to the set point. It can be seen that when the integral limit is ± 0.1 (Experiment B3_RT), process output performance improved in terms of tracking capability, with less oscillation occurring, that is, within ± 1 °C about the set point. When the integral was removed (Experiment B6_RT), response performance remained comparable to that in Experiment B3_RT.

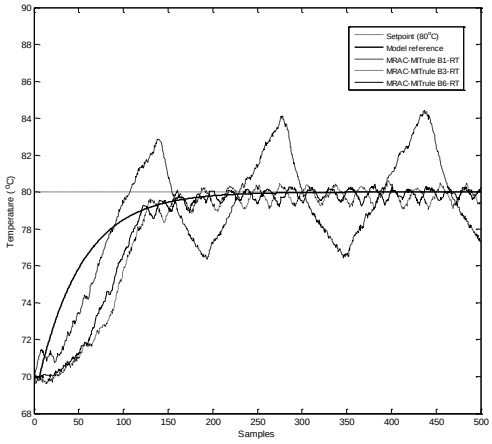

Fig. 14: Process Output using Real-time MRAC–Lyapunov Control Scheme

4.4 Simulation and real-time experimental performance comparison of MRAC (Lyapunov's theorem and MIT rule)

Figures 15 and 16 show the comparison of simulated and real-time response accuracy with respect to set point and control or actuation effort exerted during the process. Here, the evaluation involved Experiments A1, A3, and A6 for Lyapunov's theorem and B1, B3, and B6 for the MIT rule. Generally, performance accuracy, SSE, and RMSE for real-time and simulated MRAC–Lyapunov and MRAC–MIT did not show significant differences. However, SSC values differed considerably between simulated

and real-time performance. The SSC or control effort can be related to the power required to drive the actuator in the control system [18]. In real time, the actual power needed to actuate the heater was 700% to 900% greater than in the simulation due to the thermodynamics properties of the real plant, which were neglected in the simulation model. From the experiment, the MRAC–MIT achieved the lowest SSE, RMSE, and SSC in Experiment B6_RT compared to others.

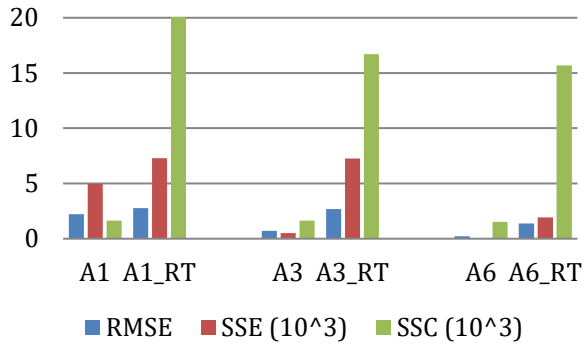

Fig. 15: Comparison Accuracy and Actuation Effort of Simulated and Real-time MRAC–Lyapunov

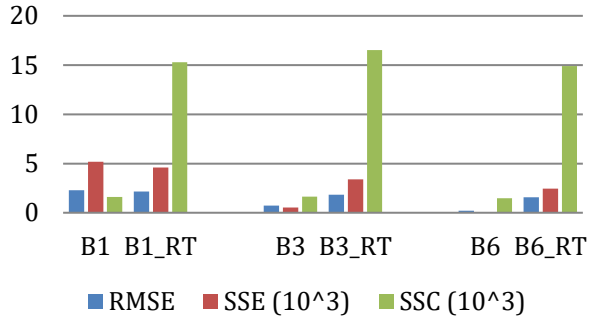

Fig. 16: Comparison Accuracy and Actuation Effort of Simulated and Real-time MRAC–MIT rule

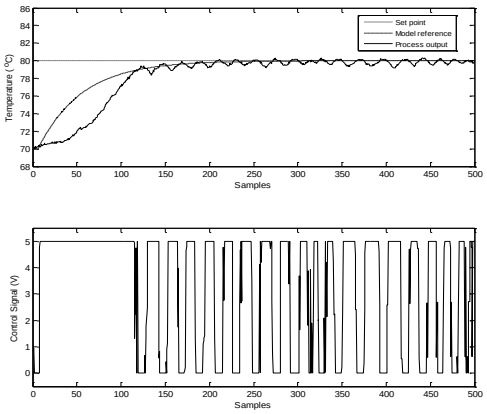

Fig. 17: Process Output and Controller Signal of Real-time MRAC–Lyapunov

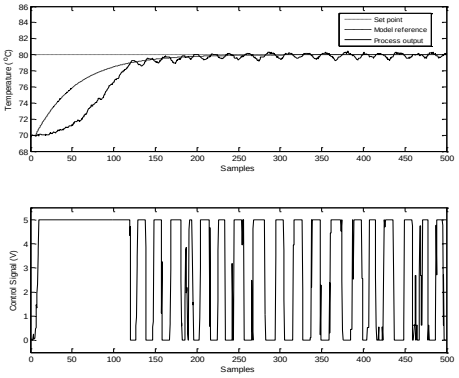

Fig. 18: Process Output and Controller Signal of Real-time MRAC–MIT

Figures 17 and 18 illustrate the performance of optimal MRAC–Lyapunov (A6_RT) and MRAC–MIT (B6_RT) controllers with their control signals respectively. From the figures, both controllers were capable in terms of tracking model reference approximately at the 200th samples until reaching a steady state with oscillation at the set point.

5. Conclusions

Temperature regulation by MRAC–Lyapunov and MRAC–MIT controllers for steam distillation was successfully applied. Table 4 shows that the MRAC–MIT controller has fast response in terms of rise time compared to the MRAC–Lyapunov controller. For peak time, there was little difference between the MIT and Lyapunov controllers at 1242s and 1271s respectively. While, the MRAC–Lyapunov response achieved settling-time faster than MRAC–MIT. However, when referring to control signals in Figure 17 and 18, both MRACs are lacking in control efficiency, as the controllers failed to maintain small actuation efforts during steady state. For future consideration, the study will extended using the Fuzzy Model Reference Learning controller (FMRLC). The FMRLC is expected to improve the efficiency of controller response and thus, reduce the effect of instantaneous change of control action that can cause wear and tear of final control element of the system.

Table 4: Controller Performance of MRAC (Lyapunov's Theorem and MIT Rule)

Controller Performance	**MRAC–Lyapunov** ***(Figure 5.31)***	**MRAC–MIT** ***(Figure 5.32)***
% of Overshoot	No overshoot	No overshoot
Rise time (s)	825	771
Peak time (s)	1271	1242
Settling time (s) 5%	1437	1583

Acknowledgements

This work has been supported by the Department of Electrical Engineering Universiti Teknologi MARA (UiTM) Shah Alam and Advanced Signal Processing Research Group (ASPRG).

Reference

[1] S. Scalia, L. Giuffreda, and P. Pallado, "Analytical and preparative supercritical fluid extraction of chamomile flowers and its comparison with conventional methods," *Journal of*

pharmaceutical and biomedical analysis, vol. 21, pp. 549-558, 1999.
[2] P. Masango, "Cleaner production of essential oils by steam distillation," *Journal of Cleaner Production*, vol. 13, pp. 833-839, 2005.
[3] S. Pourmortazavi and S. Hajimirsadeghi, "Supercritical fluid extraction in plant essential and volatile oil analysis," *Journal of Chromatography A*, vol. 1163, pp. 2-24, 2007.
[4] M. Ozel and H. Kaymaz, "Superheated water extraction, steam distillation and Soxhlet extraction of essential oils of Origanum onites," *Analytical and bioanalytical chemistry*, vol. 379, pp. 1127-1133, 2004.
[5] A. C. Kimbaris, N. G. Siatis, D. J. Daferera, P. A. Tarantilis, C. S. Pappas, and M. G. Polissiou, "Comparison of distillation and ultrasound-assisted extraction methods for the isolation of sensitive aroma compounds from garlic (Allium sativum)," *Ultrasonics sonochemistry*, vol. 13, pp. 54-60, 2006.
[6] O. Okoh, A. Sadimenko, and A. Afolayan, "Comparative evaluation of the antibacterial activities of the essential oils of Rosmarinus officinalis L. obtained by hydrodistillation and solvent free microwave extraction methods," *Journal of Food Chemistry*, vol. 120, pp. 308-312, 2009.
[7] V. J. K. M.A. McHugh, *Supercritical Fluid Extraction*. USA: Butterworth 1986.
[8] M. Khajeh, Y. Yamini, F. Sefidkon, and N. Bahramifar, "Comparison of essential oil composition of Carum copticum obtained by supercritical carbon dioxide extraction and hydrodistillation methods," *Food Chemistry*, vol. 86, pp. 587-591, 2004.
[9] D. Q. Tuan and S. G. Ilangantileket, "Liquid CO_2 extraction of essential oil from Star anise fruits (Illicium verum H.)," *Journal of Food Engineering*, vol. 31, pp. 47-57, 1997.
[10] G. Song, C. Deng, D. Wu, and Y. Hu, "Comparison of Headspace Solid-Phase Microextraction with Solvent Extraction for the Analysis of the Volatile Constituents of Leaf Twigs of Chinese Arborvitae," *Chromatographia*, vol. 58, pp. 769-774, 2003.
[11] G. Adegoke and B. Odesola, "Storage of maize and cowpea and inhibition of microbial agents of biodeterioration using the powder and essential oil of lemon grass (Cymbopogon citratus)," *International Biodeterioration & Biodegradation*, vol. 37, pp. 81-84, 1996.
[12] C. Deng, X. Xu, N. Yao, N. Li, and X. Zhang, "Rapid determination of essential oil compounds in Artemisia Selengensis Turcz by gas chromatography-mass spectrometry with microwave distillation and simultaneous solid-phase microextraction," *Analytica Chimica Acta*, vol. 556, pp. 289-294, 2006.
[13] M. Özel, F. Gö ü , J. Hamilton, and A. Lewis, "Analysis of volatile components from Ziziphora taurica subsp. taurica by steam distillation, superheated-water extraction, and direct thermal desorption with GC× GC–TOFMS," *Analytical and bioanalytical chemistry*, vol. 382, pp. 115-119, 2005.
[14] M. P. Towards, "Understanding Steam Distillation of Essential Oils by Differential Quantification of Principal Components using Capillary Gas Chromatography," PhD Thesis, University of Surrey, United Kingdom, 2001.
[15] A. Ammann, D. Hinz, R. Addleman, C. Wai, and B. Wenclawiak, "Superheated water extraction, steam distillation and SFE of peppermint oil," *Fresenius' Journal of Analytical Chemistry*, vol. 364, pp. 650-653, 1999.
[16] M. Z. Özel, F. Göğüş, J. F. Hamilton, and A. C. Lewis, "Analysis of volatile components from Ziziphora taurica subsp. taurica by steam distillation, superheated-water extraction, and direct thermal desorption with GC× GC–TOFMS," *Analytical and bioanalytical chemistry*, vol. 382, pp. 115-119, 2005.
[17] K. Astrom and B. Wittenmark, *Adaptive control*: Addison-Wesley Longman Publishing Co., Inc. Boston, MA, USA, 1994.
[18] S. Elliott, *Signal processing for active control*: Academic press, 2000.